Solid State Science and Technology, Vol. 33, No. 2 (2025) 77-86
https://doi.org/10.66514/ssst-33-2-77-86

Density Functional Theory (DFT) Study of Electronic and Structural Properties in Dy-Doped $YBa_2Cu_3O_7$ Superconductors

Rabiatul Adawiyyah Rosli[1], Azhan Hashim[2,*], Nur Hafiz Hussin[2], Siti Fatimah Saipuddin[1,3], Wan Aizuddin Wan Razali[2], Syamsyir Akmal Senawi[1]

[1]Faculty of Applied Sciences, Universiti Teknologi MARA
40450 Shah Alam, Selangor, Malaysia
[2]Faculty of Applied Sciences, Universiti Teknologi MARA Pahang, Jengka Campus,
26400 Bandar Tun Abdul Razak, Jengka, Pahang, Malaysia
[3]Ionic Materials & Devices (iMADE) Research Laboratory, Institute of Science,
Universiti Teknologi MARA, 40450 Shah Alam, Selangor, Malaysia

**Corresponding author (email: dazhan@uitm.edu.my)*

(Received: 13 October 2025 / Revised: 31 October 2025 / Accepted: 17 November 2025 / Published online: 19 November 2025)

ABSTRACT

The impact of Dy doping at the Y-site of the $Y_{1-x}Dy_xBa_2Cu_3O_{7-\delta}$ superconductor on its electronic properties was examined using Density Functional Theory (DFT) through a first-principles study. Computational simulations were performed utilizing the CASTEP computational code. The crystal structure was modelled and calculated with the Visual Crystal Approximation (VCA) employing the Generalized Gradient Approximation Perdew-Burke-Ernzerhof for Solids (GGA PBEsol) exchange-correlation and ultrasoft pseudopotential. Band structure analysis revealed the smallest bandgap at x = 0.15 between the conduction band (CB) and the valence band (VB). Electron density was found to be more concentrated near the Fermi level based on the density of states distribution. Electron density difference images displayed the merging of orbital configurations from each atom upon doping at x = 0.15. This indicates that at this specific Dy concentration, $Y_{1-x}Dy_xBa_2Cu_3O_{7-\delta}$ achieves the optimal properties.

Keywords: Superconductor; DFT, first principle; YBCO; dysprosium dopant

INTRODUCTION

The yttrium barium copper oxide $YBa_2Cu_3O_{7-\delta}$ (YBCO) is a well-known type-II superconductor that has been extensively investigated since its discovery due to its remarkable high critical temperature (T_c), which typically ranges from 70 K to 100 K [1–3]. Variations in T_c across experiments are often accompanied by corresponding changes in the critical current density (J_c), both of which are crucial parameters in understanding the resistivity and orbital behavior of superconductors. These properties ultimately determine the performance of YBCO under different operating conditions. Numerous

studies have demonstrated that doping with foreign elements can significantly alter the T_c and T_c values, thereby modifying the superconducting and structural characteristics of YBCO [4–6].

Despite extensive experimental efforts, the detailed understanding of YBCO's electronic properties, particularly its DC electrical resistivity and bandgap behavior as a function of temperature remains incomplete. This gap highlights the need for a deeper, quantum-level investigation into the influence of dopant atoms on its crystal structure and electronic configuration. The motivation of this study, therefore, lies in exploring how rare-earth doping, specifically Dy substitution at the Y-site in $Y_{1-x}Dy_xBa_2Cu_3O_{7-\delta}$, affects the electronic and structural properties of YBCO. By employing computational analysis through the CASTEP simulation tool, this work aims to predict the optimal Dy concentration that can enhance superconducting performance. Computational methods have proven effective in elucidating the structural and electronic characteristics of complex materials [7–9], thus providing valuable insight prior to experimental synthesis.

MATERIALS AND METHOD

The Cambridge Serial Total Energy Package (CASTEP) code was utilized in the computational approach of Density Functional Theory calculation for electronic analysis. Throughout the computation, the Generalized Gradient Approximation Perdew Burke Ernzerhof (GGA PBE) exchange–correlation functional have been chosen with ultrasoft pseudopotential settings. The GGA exchange-correlation has solved the over-bind atoms, which makes it a better electrical description than the exchange correlation provided by the Local Density Approximation (LDA). With the calculation setting, it mimics closely with high accuracy how the structure works. The space group, lattice parameter with atom coordinates is adopted from the works of Saipuddin et al. as the previous work using computational method using YBCO doped with Sb [1]. The variables here were used to construct the structure on the canvas of the Material Studios. To run the calculations, a High-Performance Computer (HPC) was used with the maximum values of force at 0.05 eV/Å, 0.002 Å of atom displacement, energy at 2.0×10^{-5} eV/atom with 0.1 GPa of stress. The crystal structure was optimized within 400 eV kinetic energy cut-off and k-point sampling of 4×4×1. To determine the optimum performing dopant concentration as determined by computer calculation, electronic analysis of the band structures of the pure and Dy-doped samples was done to analyze their pseudogap and density of state (DOS). Throughout the doping concentration, electronic changes were observed and documented. The percentage of Dy doped was used within the range of x = 0.00, 0.05, 0.10, 0.15 and 0.20 using the Virtual Crystal Approximation (VCA) method. The concentration of Y and Dy were adjusted according to the dopant range that was chosen using the VCA approach. These atom mixture technique selections assumed that there is a virtual atom on every possibly disordered site.

RESULTS AND DISCUSSION

In examining the effects of the GGA-PBEsol on $YBa_2Cu_3O_{7-\delta}$ superconductors, it was found that both the structural and electronic properties were changed, leading to enhanced superconducting characteristics in the materials studied. In YBCO compounds, RE

elements can substitute for both Y and Ba sites. When trivalent RE ions replace Y^{3+} and Ba^{2+}, there is a notable correlation between the solution energies and the size of the dopant which are solution energies increase for Y^{3+} and decrease for Ba^{2+} as the ionic radius grows. Smaller RE ions are energetically more favorable when substituting at the yttrium site, while larger RE ions are better suited for the barium site. Given that RE ions are similar in size to Y^{3+}, a certain degree of mixing between the yttrium and barium sites might be anticipated [10].

Structural Properties of YBCO Dy Doped

Table 1 shows the difference between lattice parameters obtained via Geometry Optimization from different concentrations (0.05, 0.10, 0.15, 0.20 and 0.25) as compared to the value obtained from pure YBCO. The closest difference of volume was obtained for concentration 0.05 which is 2.90% difference from that of pure YBCO. The minimal changes in lattice parameters suggest limited disruption to the lattice structure and potentially less impact on superconducting properties compared to other doping levels. A reduction in the dimensions a, b, or c results in smaller band gaps and a shift of the absorption edge to lower energies. Conversely, increasing a, b, or c leads to larger band gaps and a shift of the absorption edge to higher energies [11]. Furthermore, x= 0.20 and x=0.25 display substantial deviations, particularly in the c lattice parameter, with large decreases indicating pronounced distortions in the crystal structure that could lead to significant changes in superconducting characteristics. At the atomic level, this unevenness appears as a variation in the lengths of bonds between neighboring atoms. At the electronic level, the differences in element properties cause distortions in charge density. This connection implies that larger distortions in both the lattice structure and charge density are related to a greater range of material properties. This leads to the hypothesis that bigger distortions result in more significant variations in properties [12].

The a-parameter generally decreases with increasing Dy doping, although slight increases are observed at higher doping levels (x=0.20; x=0.25). This initial reduction indicates that Dy substitution leads to a contraction of the lattice along the a-axis, while the subsequent increases at elevated doping levels may result from localized structural distortions or changes in the coordination environment around the Dy ions. The parameter b exhibits a similar pattern, with a decrease followed by an increase at higher Dy concentrations, suggesting a non-linear response of the lattice parameters to Dy substitution due to competing influences of ionic size and structural modifications. In contrast, the c-parameter demonstrates a more pronounced and consistent reduction with Dy doping, particularly at higher concentrations (0.20; 0.25), where the decrease approaches 18%. This substantial reduction indicates a significant contraction of the lattice along the c-axis, likely due to the pronounced effect of Dy substitution on the interlayer spacing within the YBCO structure. Besides atomic radius, charge transfer significantly influences the local atomic distortion of elements. Research indicates that certain elements exhibit greater charge transfer, leading to more substantial displacement compared to other elements within the same composition. Elements that lose electrons tend to decrease in size, which allows for more free volume to move within their nearest-neighbor environment. Conversely, elements that gain electrons increase in size, resulting in a relatively smaller volume available for displacement [12].

Table 1. Lattice parameters and unit cell volume of pure and Dy-doped $YBa_2Cu_3O_{7-\delta}$ (x=0.05, 0.10, 0.15, 0.20 and 0.25)

Composition	Lattice Parameters		Volume	
	a (Å)	b (Å)	c (Å)	V(Å)^3
$YBa_2Cu_3O_{7-\delta}$ [1]	3.827353	3.906071	11.609807	173.565548
$YBa_2Cu_3O_{7-\delta}$	3.847773	3.909941	11.609249	174.656097
$Y_{0.95}Dy_{0.05}Ba_2Cu_3O_{7-\delta}$	3.809810 (0.99%)	3.886464 (0.60%)	11.454148 (1.34%)	169.598045 (2.90%)
$Y_{0.90}Dy_{0.10}Ba_2Cu_3O_{7-\delta}$	3.760644 (2.26%)	3.797668 (2.87%)	11.481820 (1.10%)	163.979655 (6.11%)
$Y_{0.85}Dy_{0.15}Ba_2Cu_3O_{7-\delta}$	3.662685 (4.81%)	3.711429 (5.08%)	11.477377 (1.14%)	156.021112 (10.67%)
$Y_{0.80}Dy_{0.20}Ba_2Cu_3O_{7-\delta}$	3.990065 (3.70%)	4.067640 (4.03%)	9.522271 (17.98%)	154.547866 (11.51%)
$Y_{0.75}Dy_{0.25}Ba_2Cu_3O_{7-\delta}$	3.871099 (0.61%)	3.934099 (0.62%)	9.578602 (17.49%)	145.875254 (16.48%)

Band Structure and Energy Gap of Dy Doped YBCO

Figures 1(a) - 1(e) show an electronic analysis of both pure and Dy-doped samples in the Y-site of $YBa_2Cu_3O_7$-δ revealed alterations in the pseudogap band structure above the Fermi level. Doping yttrium barium copper oxide (YBCO) with dysprosium (Dy) at the Y site involves substituting some of the Yttrium (Y) atoms in the YBCO crystal lattice with dysprosium (Dy) atoms. This substitution can significantly affect the material's electronic properties, particularly its pseudogap behavior. The substitution of Dy^{3+} ions for Y^{3+} ions possibly introduce differences in the electronic state in the CuO_2 plane and affects the transition temperature T_c [10]. Doping YBCO with Dy at the Y site leads to changes in the pseudogap values, reflecting alterations in its electronic structure.

Table 2 shows pseudogap value for Dy-doped $Y_{1-x}Dy_xBa_2Cu_3O_{7-\delta}$ (x=0.05, 0.10, 0.15, 0.20 and 0.25). For compositions with Dy content from concentration 0.05 to 0.15, the pseudogap value decreases as Dy content increases, suggesting a reduction in the energy required for the pseudogap state, which potentially affects the electronic states and density of states in the material. However, at higher Dy concentrations $x > 0.20$ the pseudogap value increases again, indicating a more complex interaction between Dy atoms and the YBCO lattice. The pseudogap is influenced by doping and has a momentum dependence similar to that of the d-wave superconducting gap. In the normal state of underdoped cuprates, the pseudogap reduces the density of states at the Fermi level, which can, in turn, impact the transition temperature and the isotope effect coefficient α in cuprates. Experimental evidence shows that the pseudogap exists in both underdoped and overdoped samples and can be correlated with the superconducting gap [13]. These changes can significantly affect superconducting properties, such as the transition temperature T_c, critical current density, and magnetic properties, making it possible to optimize YBCO's properties for specific applications.

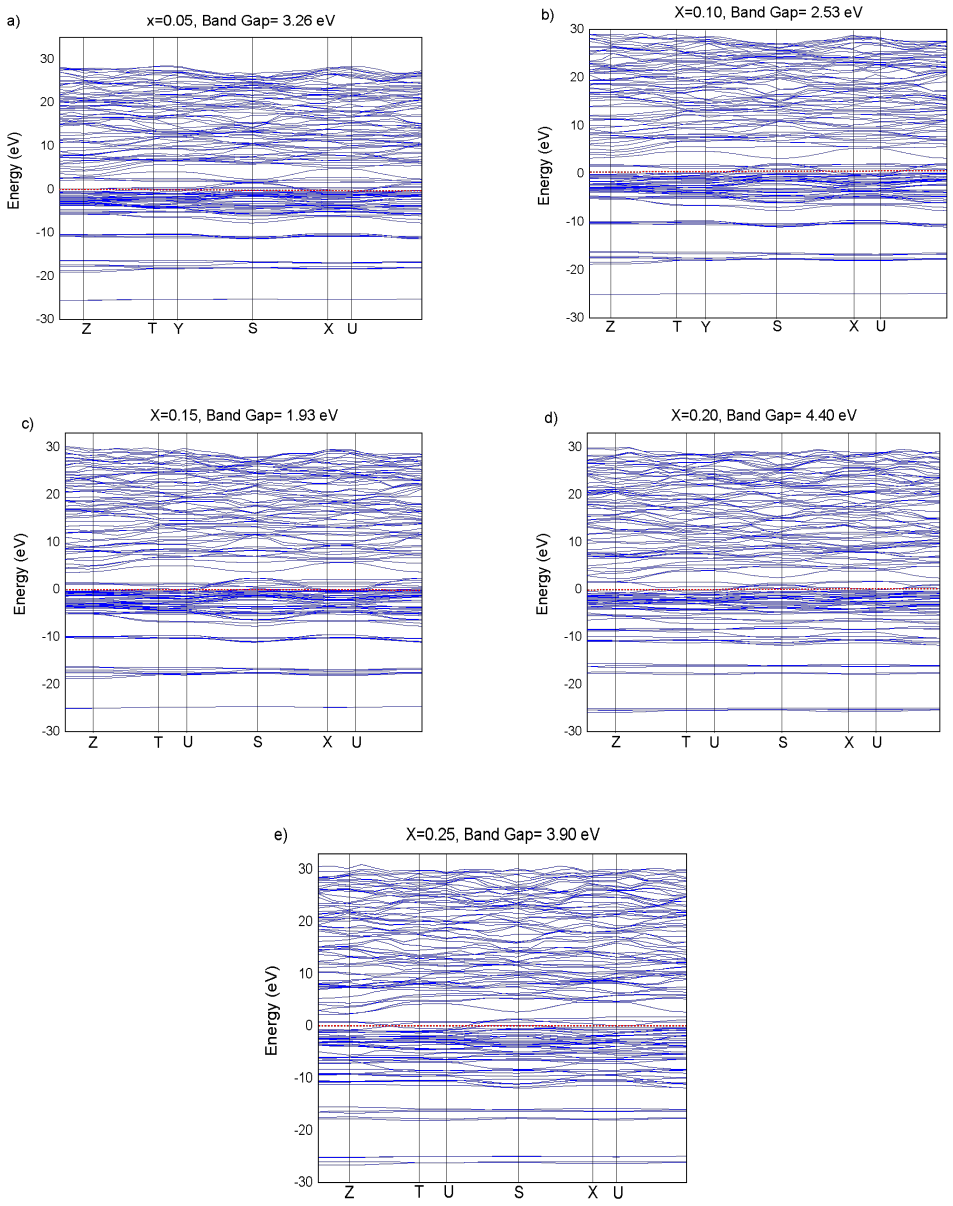

Figure 1. Band structure for for Dy-doped $Y_{1-x}Dy_xBa_2Cu_3O_{7-\delta}$ (a) x=0.05, (b) x=0.10, (c) x=0.15, (d) x=0.20 and (e) x=0.25

Table 2. Pseudogap value for Dy-doped $Y_{1-x}Dy_xBa_2Cu_3O_{7-\delta}$ (x=0.05-0.25)

Composition	Pseudogap value (eV)
$Y_{0.95}Dy_{0.05}Ba_2Cu_3O_{7-\delta}$	3.26
$Y_{0.90}Dy_{0.10}Ba_2Cu_3O_{7-\delta}$	2.53
$Y_{0.85}Dy_{0.15}Ba_2Cu_3O_{7-\delta}$	1.93
$Y_{0.80}Dy_{0.20}Ba_2Cu_3O_{7-\delta}$	4.40
$Y_{0.75}Dy_{0.25}Ba_2Cu_3O_{7-\delta}$	3.90

In high-temperature superconductors (HTSCs), the single-electron density of states (DOS) notably decreases at temperatures significantly higher than the superconducting transition temperature, over a wide range of temperatures above T_c. This effect is known as a pseudogap [14]. As the doping concentration increases from $x = 0.05$ to $x = 0.15$, the band gap decreases from 3.26 eV to 1.93 eV. This trend suggests that the introduction of Dy atoms into the host lattice creates localized states within the band gap, which facilitate electronic transitions at lower energies [15]. The increased number of Dy atoms likely leads to enhanced interaction and overlapping of these states, effectively reducing the band gap. The reduction of the band gap increases, highlighting the significant influence of the atomic number on the band gap reduction due to its associated electron configuration. Therefore, it can be inferred that as the shell radius increases, the degree of band gap reduction decreases [16]. At $x = 0.20$, there is a notable increase in the band gap to 4.4 eV. This unexpected jump can be attributed to several factors. One possible explanation is the formation of Dy-related defect states that modify the electronic structure more significantly. Zhou et al. mentioned when exposed to an external magnetic field, these defects function as non-superconducting regions that hinder the movement of magnetic flux quanta within the superconductor [17]. This reduces the system's overall energy and helps preserve the material's superconductivity. If the defect size is roughly twice the coherence length of YBCO, it can effectively pin vortices. However, if the defect size becomes too large, reducing the superconducting volume within the film, it can significantly diminish the film's current-carrying capacity and potentially result in a loss of superconducting properties [17,18]. Another consideration is the potential phase change or structural transformation in the material, which can lead to a different electronic band structure and hence a higher band gap. When the doping concentration reaches $x = 0.25$, the band gap decreases again to 3.9 eV. This reduction may result from the saturation of defect states or a partial return to a previous structural phase, reducing the influence of Dy-induced modifications. The balance between the creation of new states and the stabilization of existing ones could lead to the observed band gap value. Y123 conductivity can be attributed to the influence of the energy band originating from the Cu–O chain. This conductive behavior is likely due to the charge transfer dynamics associated with this specific energy band, which facilitates electron movement and enhances the compound's conductive properties. Another notable feature of YBCO is its high anisotropy. With Y atoms being insulated, the two Cu-O_2 planes create a dielectric-like layer. Given YBCO's layered structure, its resistivity along the *c*-axis is typically higher than in the *a*-*b* plane. Additionally, the oxygen atoms doped into the Cu–O chains introduce extra holes and electronic connections along the b-axis (or b2 reciprocal vector) of the system [19].

Density of States of Dy Doped YBCO

The density of states (DOS) for Dy-doped YBCO at concentrations of $x = 0.05$, 0.10, 0.15, 0.20, and 0.25 is illustrated in Table 3. Initially, from x=0.05 to x=0.10, there is a slight decrease in total energy, suggesting a minor reduction in the overall population of energy states. However, as the Dy concentration increases beyond x=0.10, there is a noticeable increase in total energy, peaking at x=0.25. This indicates a growing number of available electronic states at higher energies which mean the increase in the dielectric constant observed with decreasing atomic size is believed to be due to the rise in state

density [19]. The contribution of s-orbital energy significantly decreases with higher Dy concentrations, dropping from 12.60 eV at x=0.05 to 7.50 eV at x=0.25. This decline shows that s-orbital states become less dominant in the DOS with more Dy. In contrast, p-orbital energy peaks at x=0.10 with 13.30 eV, then diminishes at higher concentrations, suggesting that p-orbital states are more significant at intermediate Dy levels but less so as the concentration increases further, possibly due to changes in hybridization or bonding interactions. Furthermore, the d-orbital energy contribution consistently rises from 9.63 eV at x=0.05 to 14.70 eV at x=0.25, reflecting the increasing importance of d-orbital states in the DOS as Dy concentration increases. This trend is expected since Dy, being a transition metal, has partially filled d-orbitals, and its increasing concentration naturally leads to a higher density of d-states.

Table 3. Density of states for Dy-doped $Y_{1-x}Dy_xBa_2Cu_3O_{7-\delta}$ (x=0.05 to 0.25)

Dy concentration	Sum (eV)	s (eV)	p (eV)	d (eV)
x= 0.05	17.10	12.60	7.37	9.63
x= 0.10	16.90	7.81	13.30	10.00
x= 0.15	16.60	8.21	13.00	10.80
x= 0.20	18.40	10.10	10.10	13.70
x= 0.25	20.20	7.50	9.78	14.70

Figure 2 shows that at lower doping levels (x = 0.05 and x = 0.10), the total DOS (sum) decreases slightly from 17.10 eV to 16.90 eV. The s-orbital contribution decreases from 12.60 eV to 7.81 eV, while the p-orbital contribution increases from 7.37 eV to 13.30 eV, and the d-orbital contribution increases marginally from 9.63 eV to 10.00 eV. This implies that at x = 0.10, there are more states available in the p-orbitals, suggesting that the p-orbital states are contributing more to the conduction band, thereby enhancing the material's electrical conductivity [20]. As the doping level increases to x = 0.15, the total DOS slightly decreases to 16.60 eV. Here, the s-orbital contribution rises to 8.21 eV, the p-orbital contribution slightly drops to 13.00 eV, and the d-orbital contribution increases to 10.80 eV. This indicates a redistribution of states among the orbitals, with d-orbital states becoming more significant, possibly contributing to both the conduction and valence bands.

At x = 0.20, the total DOS increases to 18.40 eV, with a noticeable rise in the s-orbital contribution to 10.10 eV, a significant reduction in the p-orbital contribution to 10.10 eV, and a marked increase in the d-orbital contribution to 13.70 eV. Finally, at the highest doping level of x = 0.25, the total DOS peaks at 20.20 eV. The s-orbital contribution drops significantly to 7.50 eV, the p-orbital contribution remains relatively stable at 9.78 eV, and the d-orbital contribution further increases to 14.70 eV. This indicates a dominant role of d-orbitals in both conduction and valence bands, with d-orbital states significantly contributing to the material's electronic properties. In summary, the changes in the density of states with varying Dy doping concentrations reveal a complex interaction between s-, p-, and d-orbital contributions. At lower doping levels, p-orbitals dominate the conduction processes, while at higher doping levels, d-orbitals become increasingly significant. This behavior can be related to the narrowing of

the pseudogap and the shifting of electronic states towards the Fermi level, affecting the material's conductivity and overall electronic properties.

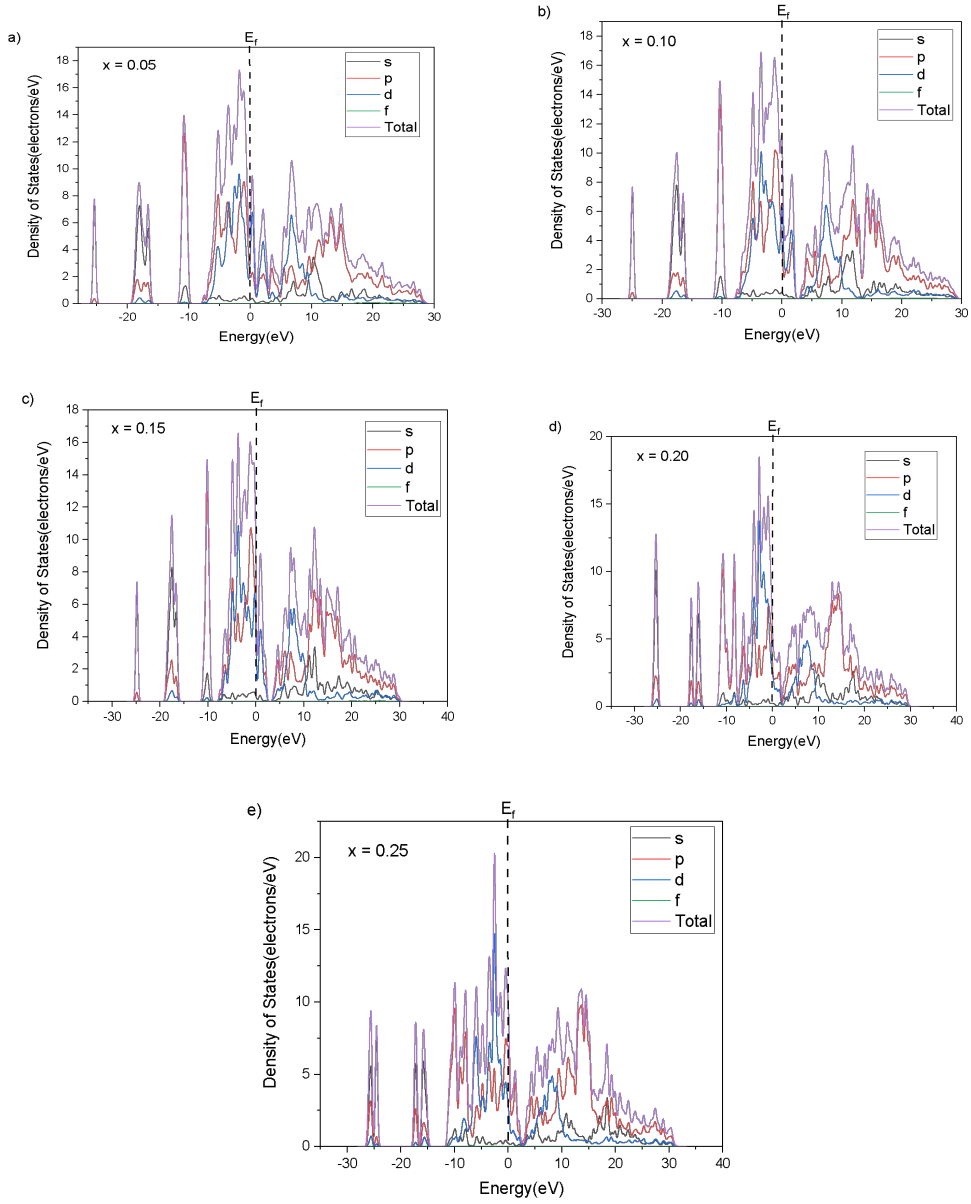

Figure 2. Density of States for for Dy-doped $YBa_2Cu_3O_{7-\delta}$ (a) x=0.05; (b) x=0.10; (c) x=0.15; (d) x=0.20; (c) x=0.25

CONCLUSIONS

Ultimately, Dy dopant at x = 0.15 on the Y-site of YBCO exhibits ideal superconducting characteristics. These were noted from the density of states, electron density difference, and pseudogap at different locations inside the structure. The electron mobility was facilitated by the 1.93 eV band structure pseudogap between the valence and conduction bands. According to the density of states graph, the DOS rises and shifts in the direction

of the Fermi level as the dopant increases. The maximum electron density is likewise seen in PDOS for both the Cu 3d and O 2p orbitals at $x = 0.15$ for the Dy dopant and the closest to the fermi level. When the amount of Dy dopant grows at the structure's Y-site, the electron density differential along the Y-site indicates the increase in electron density. Since a tiny portion of the doping concentration can be virtually conducted. Using the first principles method, more data may be collected before actual building is carried out through experimental work. This could encourage the complete utilization of raw materials and green technologies also saves time to conduct the experiment.

ACKNOWLEDGEMENTS

The financial support from the Ministry of Higher Education Malaysia (MOHE) through the Fundamental Research Grant Scheme (FRGS), project number FRGS/1/2022/STG07/UITM/01/1, is gratefully acknowledged. We also extend our appreciation to Universiti Teknologi MARA Pahang and the Ionic Materials & Devices (iMADE) Research Laboratory at the Institute of Science, Universiti Teknologi MARA, Shah Alam, for providing the research facilities.

CONFLICT OF INTEREST STATEMENT

The authors agree that this research was conducted in the absence of any self-benefits, commercial or financial conflicts and declare absence of conflicting interests with the funders.

REFERENCES

1. Saipuddin SF, Rosli NH, Azhan H, Nurbaisyatul ES, Taib MFM. Effect of Sb-doped $YBa_{2-x}Sb_xCu_3O_{7-\delta}$ superconductor on electronic behaviour using density functional theory. *Cryogenics*. 2020;111:103175.
2. Talantsev EF and Tallon JL. Universal self-field critical current for thin-film superconductors. *Nature Communication*. 2015;6:1-8.
3. Tavana A and Akhavan M. How T_C can go above 100 K in the YBCO family. *European Physical Journal B*. 2010;73(1):79–83.
4. Augieri A, Petrisor T, Celentano G, Ciontea L, Galluzzi V, Gambardella U, Mancini A, Rufoloni A. Effect of Ca doping in YBCO superconducting thin films. *Physica C Superconductivity.* 2004;401(1-4):320–324.
5. Yao X, Oka A, Izumi T, Shiohara Y. Crystal growth and superconductivity of Fe-doped YBCO single crystals. *Physica C: Superconductivity and its Applications*. 2000;339(2): 99–105.
6. Shlyk L, Krabbes G, Fuchs G, Nenkov K. Melt-processed YBCO doped with Ca and Cd: comparison of superconducting properties. *Physica C: Superconductivity.* 2002;383(1-2):175-182.
7. Saipuddin SF, Hashim A, Samat MH, Suhaimi NE, Taib MFM. DFT+U calculation in determining structural and electronic properties of $YBa_2Cu_3O_{7-d}$. *AIP Conf. Proc.* 2021;2368:040001.
8. Yücel İ, Çakmak S. The role of carbon (C) atoms on YBCO superconductor: DFT study. *Optoelectronics and Advanced Materials-Rapid Communications.*

2017;11(9):590–599.
9. Helal MA, Farid Ul Islam AKM, Liton MNH, Kamruzzaman M. Hydrostatic pressure dependent structural, elastic, vibrational, electronic, and optoelectronic properties of superconducting $BaCuO_3$: A DFT insight. *Journal of Physics and Chemistry of Solids.* 2022;161:110452.
10. Öztürk A, Doğan M, Düzgün İ, Çelebi S. The Effect of Dy Doping on the Magnetic Behavior of YBCO Superconductors. *Journal of Superconductivity and Novel Magnetism*. 2016;29(7):1787–1791.
11. Shohonov DA, Migas DB, Filonov AB, Borisenko VE, Takabe R, Suemasu T. Effects of lattice parameter manipulations on electronic and optical properties of $BaSi_2$. *Thin Solid Films*. 2019;686:137436.
12. Aidhy DS. Chemical randomness, lattice distortion and the wide distributions in the atomic level properties in high entropy alloys*, Computational Materials Science*. 2024;237:112912–112912.
13. Tewari BS, Ahlawat M, Dhyani A, Ajay. Influence of pseudo-gap and interlayer coupling on isotope effect in bilayer cuprate superconductors. *Physica C: Superconductivity*. 2021;587:1353895–1353895.
14. Hannachi E, Slimani Y, Almessiere MA, Alotoibi SA, Omelchenko LV, Petrenko EV, Kurbanov U, Ben Azzouz F, Solovjov AL, Baykal A. YBCO polycrystal co-added with $BaTiO_3$ and WO_3 nanoparticles: Fluctuation induced conductivity and pseudogap studies. *Current Applied Physics*. 2023;48:70–78.
15. Kurboniyon M S, Lou B, Zafari U, Rahimi F, Srivastava AM, Yamamoto T, Brik MG, Ma C.-G. First-principles study of geometric and electronic structures, and optical transition energies of Mn^{4+} impurity ions: K_2SiF^6 as a prototype. *Journal of Luminescence*. 2023;263:120103–120103.
16. Ahmed TY, Aziz SB, Dannoun EMA. Role of Outer shell Electron-Nuclear Distant of Transition Metal Atoms (TMA) on Band Gap Reduction and Optical Properties of TiO_2 Semiconductor. *Results in Engineering*. 2024;23:102479–102479.
17. Zhou X, Chen J, Huang R, Liu Z, Cai C. Effects of $BaCO_3$ in transient liquid-assisted fluorine-free metal organic deposition on the growth process of YBCO. Colloids and Surfaces a Physicochemical and Engineering Aspects. 2024;691:133830–133830.
18. Trabelsi Y, Segovia-Chaves F, Ben Ali N. Tunable defect modes through the (YBCO-Yttria) based on Octonacci photonic quasicrystals. *Results in Physics.* 2023;44:106176–106176.
19. Cheong CM, Chen SK. First principal calculation of electronic structures and hole concentration of YBCO family compounds. *Materials Today Proceedings*. 2024;96:94–99.
20. Zhang X, Song Y, Zhou D, Li T, Wang X, Huang H, Tang R, Zeng P, Wu X, Deng Z. Influence of Ag Doping on Thermal Conductivity and Magnetic Levitation of Single Grain YBCO Superconductors for High-Temperature Superconducting Maglev. *Cryogenics.* 2024;137:103774–103774.